ASTRONOMY & ASTROPHYSICS
SUPPLEMENT SERIES

Astron. Astrophys. Suppl. Ser. **111,** 347-357 (1995)

Atomic data from the IRON Project. X. Effective collision strengths for infrared transitions in silicon- and sulphur-like ions

M.E. Galavís[1], C. Mendoza[2] and C.J. Zeippen[3]

[1] Departamento de Física, Universidad Metropolitana, PO Box 76819, Caracas 1070A, Venezuela
[2] Centro de Física, Instituto Venezolano de Investigaciones Cientifícas (IVIC), PO Box 21827, Caracas 1020A, Venezuela
[3] UPR 261 du CNRS et DAMAp and URA 173 (associée au CNRS et à l'Université Paris 7) et DAEC, Observatoire de Paris, F-92195 Meudon, France

Received September 23, 1994; accepted January 3, 1995

Abstract. — Effective collision strengths for the electron impact excitation of transitions within the $3s^2 3p^q$ ground configuration of ions in the silicon ($q = 2$) and sulphur ($q = 4$) isoelectronic sequences are presented. We consider here astrophysically abundant ions that give rise to infrared transitions within their ^3P_J ground term, namely, S III, Cl IV, Ar V, K VI, Ca VII, Ar III, K IV and Ca V. The configuration-interaction target approximations developed for the R-matrix calculations include single and double excitations within the $n = 3$ complex. An attempt is made to include a sufficient number of $n = 3$ target states in the close-coupling expansion so as to account for the prominent resonance effects that dominate the energy regions of interest, but development is handicapped since the energies of many of these states have not been measured. The contributions from resonances converging to $n = 4$ target states, which begin to appear in the energy region of interest for the lower members of the sequence, are studied in the case of S III. Relativistic effects in the target, which become important for high Z, are examined in Ca V. Both of these contributions to the excitation cross sections are found to be relatively small (< 20%) and therefore are neglected in the other systems under consideration. The good agreement found with previous calculations for S III and Ar III suggests that the present collisional data for the weakly ionised members of the sequence may be accurate to within 20%, but we expect this rating to deteriorate for higher Z due to the neglect of extra contributing thresholds.

Key words: atomic and molecular data — infrared: general

1. Introduction

The IRON Project (Hummer et al. 1993, hereafter Paper I) is an international collaboration established to compute collisional and radiative data for ions of astrophysical interest, in particular for the heavier species in the iron group. In this respect, the first phase of the Project is concerned with the calculation of electron impact excitation rates for modeling infrared (IR) lines which are used in plasma diagnostics (see also earlier papers in the present series by Lennon & Burke 1994; Zhang et al. 1994; Saraph & Tully 1994; Butler & Zeippen 1994; Zhang & Pradhan 1995; Nahar 1995; Berrington 1995; Pelan & Berrington 1995). Although accurate astronomical observations of such lines have been difficult in the past, forthcoming missions involving satellite-borne telescopes such as the Infrared Space Observatory (ISO) and the Space Infrared Telescope Facility (SIRTF) are likely to change this situation. Furthermore, as shown in the critical compilations by Mendoza (1983); Pradhan & Gallagher (1992); Lang (1994) and references therein, the electron impact excitation rates that will be required for many ionic species have only been calculated previously using unreliable approximations; therefore, a major revision has been suggested using the more accurate approaches currently available, e.g., the R-matrix method of Burke et al. (1971). Regarding the silicon and sulphur isoelectronic sequences which are part of our present interests, only S III and Ar III are believed to have been treated with reliable accuracy (see Mendoza 1982 and Johnson & Kingston 1990, respectively).

Within the context of the IRON Project, we present here electron impact excitation rates for transitions in the ground configuration of astrophysically abundant ions of the silicon (S III, Cl IV, Ar V, K VI, Ca VII) and sulphur

Send offprint requests to: C.J. Zeippen

(Ar III, K IV and Ca V) sequences. These ions give rise to infrared (IR) transitions within their ^3P_J ground term. Wavefunctions for target states are generated in a configuration interaction (CI) scheme, and the electron impact excitation collision strengths have been computed by the R-matrix method attempting to include a sufficient number of target states in the close-coupling (CC) expansion (Burke & Seaton 1971) to account for the resonances that dominate the energy regions of interest; however, this requirement can be only partially fulfilled due to incompleteness in the measured spectra for these ions. This problem is particularly acute in Fe XI and Fe XIII which require much larger target descriptions than those considered in the present work. Calculations for these systems are currently in progress and will be reported elsewhere. In Sect. 2 the present numerical method is briefly described; in Sect. 3 we give the target approximations used in the computations, followed by discussions of the results in Sects. 4 and 5.

2. Numerical method

The numerical methods used in the present calculations have been described in detail in Paper I of the present series. They are based on the CC method of scattering theory (Burke & Seaton 1971) where an $(N+1)$-electron ionic system is described in terms of an N-electron parent ion (usually referred to as the *target*) and an incident electron. Wavefunctions for the total system are thus expanded in terms of the target eigenfunctions

$$\Psi^{SL\pi} = \mathcal{A}\sum_i \chi_i\theta_i + \sum_j c_j\Phi_j \ , \qquad (1)$$

where $\mathcal{A}$ is the antisymmetrisation operator, χ_i are the target eigenfunctions and θ_i are the incident-electron functions. The Φ_j are bound-state type functions for the total system introduced to compensate for orthogonality conditions imposed on the θ_i and to render short-range correlation. The application of the Kohn variational principle with the θ_i functions and the coefficients c_j as variational parameters leads to a set of integro-differential equations that are solved numerically. LS-coupling is assumed throughout, and therefore, states of the total N-electron ionic system are assigned the quantum numbers $SL\pi$ (total spin, orbital angular momentum and parity). The integro-differential equations obtained from the Kohn variational principle are solved with codes based on the R-matrix method (Burke et al. 1971) and on new asymptotic techniques developed by Seaton (1985).

Following Saraph (1972, 1978), collision strengths for fine-structure transitions are obtained by algebraic recoupling of the $SL\pi$ reactance matrices to intermediate coupling

$$K^{J\pi}(S_1L_1J_1l_1k_1, S_2L_2J_2l_2k_2) = \sum_{SL} K^{SL\pi}(S_1L_1l_1s_1, S_2L_2l_2s_2)\, C(SLJ, S_1L_1J_1, l_1k_1)C(SLJ, S_2L_2J_2, l_2k_2) \ , \qquad (2)$$

where the C algebraic coefficients can be expressed in terms of Racah coefficients. Here the total angular momentum of the target, J_i, is coupled to the orbital angular momentum, l_i, and spin, s_i, of the incident electron via an intermediate quantum number, k_i,

$$\mathbf{J_i} + \mathbf{l_i} = \mathbf{k_i} \qquad \text{and} \qquad \mathbf{k_i} + \mathbf{s_i} = \mathbf{J} \qquad (3)$$

to form states of the total system with quantum numbers $J\pi$. Furthermore, relativistic effects in the target can be included to first order by the second transformation

$$K^{J\pi}(\Delta_1J_1k_1, \Delta_2J_2k_2) = \sum_{S_1L_1S_2L_2} K^{J\pi}(S_1L_1J_1k_1, S_2L_2J_2k_2)\, f_{J_1}(S_1L_1, \Delta_1)f_{J_2}(S_2L_2, \Delta_2) \ , \qquad (4)$$

where the f coefficients are referred to as term-coupling coefficients (Jones 1975). In the present work such transformations have been performed with a new extended version of the asymptotic code developed by Pradhan & Zhang (1994).

For electron collisional de-excitation (a downward transition $i \rightarrow j$ with $i > j$), the rate coefficient is given by the expression

$$q_{ij}(T) = \frac{8.631\ 10^{-6}\Upsilon_{ij}(T)}{\omega_i T^{1/2}} \quad \mathrm{cm^3 s^{-1}} \ , \qquad (5)$$

where the effective collision strength $\Upsilon_{ij}(T)$ is obtained by convoluting the collision strength for the transition, $\Omega_{ij}(E)$, with a Maxwellian distribution

$$\Upsilon_{ij}(T) = \int_0^\infty \Omega_{ij}(E_i)\exp(-E_i/\kappa T)\mathrm{d}(E_i/\kappa T) \ . \qquad (6)$$

Here E_i is the energy of the incident electron (in Ryd) relative to the ith level, T is the electron temperature in K, ω_i is the statistical weight of the ith level and κ is the Boltzmann constant. For collisional excitation ($j \rightarrow i$), the rate coefficient can be obtained from the relation

$$q_{ji} = (\omega_i/\omega_j)\exp[-\Delta E_{ij}/\kappa T]q_{ij} \qquad i > j \ . \qquad (7)$$

where ΔE_{ij} is the level energy separation. In the present work, collision strengths are computed in a mesh with a constant energy interval fine enough to delineate the resonance structure.

Table 1. Scaling parameters of the Thomas-Fermi statistical model potential used to generate the target orbitals

Ion	λ_{1s}	λ_{2s}	λ_{2p}	λ_{3s}	λ_{3p}	λ_{3d}	λ_{4s}
S III	1.4562	1.0910	1.0358	1.0903	1.0906	1.1732	1.1276
Cl IV	1.4463	1.0959	1.0397	1.0978	1.0924	1.1550	
Ar V	1.4448	1.0992	1.0428	1.1052	1.0946	1.1443	
K VI	1.4407	1.1027	1.0455	1.1113	1.0969	1.1378	
Ca VII	1.4295	1.1059	1.0478	1.1155	1.0989	1.1338	
Ar III	1.4428	1.1046	1.0482	1.1069	1.1064	1.1695	
K IV	1.4482	1.1091	1.0507	1.1148	1.1081	1.1570	
Ca V	1.4362	1.1114	1.0529	1.1215	1.1113	1.1551	

Table 2. Comparison of theoretical and experimental term energies for the S III target description. The latter were obtained from the recent compilation by Martin et al. (1990). It can be seen that there are three terms that have not been observed

State	E_{th} (Ryd)	E_{expt} (Ryd)
$3s^23p^2\ ^3P$	0.0	0.0
$3s^23p^2\ ^1D$	0.1165	0.0981
$3s^23p^2\ ^1S$	0.2601	0.2424
$3s3p^3\ ^5S^0$	0.4912	0.5295
$3s3p^3\ ^3D^0$	0.7562	0.7610
$3s3p^3\ ^3P^0$	0.8930	0.8949
$3s^23p3d\ ^1D^0$	0.9584	0.9441
$3s^23p3d\ ^3F^0$	1.1364	
$3s3p^3\ ^1P^0$	1.3023	1.2419
$3s3p^3\ ^3S^0$	1.2945	1.2530
$3s^23p3d\ ^3P^0$	1.3364	1.2991
$3s^23p4s\ ^3P^0$	1.3620	1.3341
$3s^23p3d\ ^3D^0$	1.3809	1.3407
$3s^23p4s\ ^1P^0$	1.3999	1.3472
$3s3p^3\ ^1D^0$	1.4484	1.3798
$3s^23p3d\ ^1F^0$	1.5189	
$3s^23p3d\ ^1P^0$	1.5899	

Table 3. Comparison of theoretical and experimental term energies for the Ca V target. The spectroscopic values are from the compilation by Sugar & Corliss (1979). It can be seen that target model development is limited by the few measurements that have been reported, particularly when adjusting the thresholds at the measured values in order to get as accurate a resonance pattern as possible

State	$E_{\rm th}$ (Ryd)	$E_{\rm expt}$ (Ryd)
$3s^23p^4\ ^3P$	0.0	0.0
$3s^23p^4\ ^1D$	0.1728	0.1610
$3s^23p^4\ ^1S$	0.3896	0.3889
$3s3p^5\ ^3P^0$	1.3919	1.4085
$3s3p^5\ ^1P^0$	1.8226	1.7923
$3s^23p^33d\ ^5D^0$	1.9125	
$3s^23p^33d\ ^3D^0$	2.0719	
$3s^23p^33d\ ^1S^0$	2.1292	
$3s^23p^33d\ ^3F^0$	2.1606	
$3s^23p^33d\ ^3G^0$	2.3011	
$3s^23p^33d\ ^1G^0$	2.3491	
$3s^23p^33d\ ^1D^0$	2.3769	2.3052
$3s^23p^33d\ ^3F^0$	2.4898	
$3s^23p^33d\ ^3P^0$	2.4974	
$3s^23p^33d\ ^3D^0$	2.5005	
$3s^23p^33d\ ^1F^0$	2.6807	2.5770
$3s^23p^33d\ ^3S^0$	2.8482	2.6666
$3s^23p^33d\ ^1P^0$	2.8175	2.7431
$3s^23p^33d\ ^3P^0$	2.8191	
$3s^23p^33d\ ^3D^0$	2.9727	2.8078
$3s^23p^33d\ ^1D^0$	3.0944	2.8940
$3p^6\ ^1S$	3.1095	
$3s^23p^33d\ ^1F^0$	3.1713	2.9896
$3s^23p^33d\ ^1P^0$	3.3516	3.2082

3. Target approximations

Wavefunctions for the ionic targets are calculated in a Thomas-Fermi statistical model potential $V(r/\lambda; Z, N)$ with the atomic structure program SUPERSTRUCTURE (Eissner et al. 1974; Nussbaumer & Storey 1978; Eissner 1991). For generating the radial orbitals, P_{nl}, the corresponding λ_{nl} scaling parameters are optimized by minimizing a weighted sum of the energies of the terms that are included in the chosen target approximation. For the Si-like ions, a 15-state approximation is adopted; that is, all terms arising from the configurations $3s^23p^2$, $3s3p^3$ and $3s^23p3d$. For ions in the S sequence, the 24 terms belonging to the configurations $3s^23p^4$, $3s3p^5$, $3s^23p^33d$ and $3p^6$ are included. Configuration interaction (CI) is limited to single and double excitations within the $n = 3$ complex of the states included in the target representations. The optimized scaling parameters for each system are given in Table 1. For the case of S III, a more elaborate approximation is also considered whereby the two $3s^23p4s\ ^{3,1}P^\circ$ terms, embedded among states of the $3s3p^3$ and $3s^23p3d$ excited configurations (see Table 2), are also included in the target representation. This approximation also includes implicitly extra CI through correlation configurations with 4s orbitals.

In order to obtain the resonance positions as accurately as possible, the collision calculations are performed using, whenever possible, the experimental target-term energy separations compiled in the literature: Martin et al. (1990) for S III; Moore (1971) for Cl IV, Ar III and Ar V; Corliss & Sugar (1979) for K IV and K VI and Sugar & Corliss (1979) for Ca V and Ca VII. However, as illustrated in Table 3 for the case of Ca V, the number of observed terms for Si- and S-like ions is generally scanty, which seriously limit the accuracy and completeness of the target descriptions that can be obtained.

Table 4. Effective collision strengths for transitions within the $3s^2 3p^2$ ground configuration of S III

	Transition					
$\log T$ (K)	$^3P_0-^3P_1$	$^3P_0-^3P_2$	$^3P_1-^3P_2$	$^3P-^1D$	$^3P-^1S$	$^1D-^1S$
3.0	1.702	0.808	3.947	6.023	1.372	1.094
3.2	1.855	0.815	4.153	6.932	1.297	1.037
3.4	1.993	0.870	4.449	7.689	1.214	0.984
3.6	2.153	0.961	4.854	8.038	1.150	0.982
3.8	2.290	1.042	5.208	8.023	1.117	1.093
4.0	2.331	1.110	5.411	7.951	1.110	1.301
4.2	2.278	1.207	5.563	7.989	1.131	1.540
4.4	2.185	1.327	5.716	8.006	1.193	1.772
4.6	2.078	1.413	5.776	7.829	1.261	1.962
4.8	1.933	1.413	5.594	7.332	1.257	2.054
5.0	1.716	1.308	5.088	6.478	1.146	2.016

Table 5. Effective collision strengths for transitions within the $3s^2 3p^2$ ground configuration of Cl IV

	Transition					
$\log T$ (K)	$^3P_0-^3P_1$	$^3P_0-^3P_2$	$^3P_1-^3P_2$	$^3P-^1D$	$^3P-^1S$	$^1D-^1S$
3.0	2.694	2.040	7.956	9.272	1.743	0.697
3.2	2.672	2.054	7.961	8.872	1.733	0.717
3.4	2.579	2.078	7.899	8.272	1.718	0.743
3.6	2.376	2.046	7.574	7.527	1.721	0.803
3.8	2.099	1.927	6.959	6.856	1.780	0.960
4.0	1.828	1.753	6.229	6.437	1.922	1.240
4.2	1.645	1.592	5.639	6.337	2.089	1.578
4.4	1.595	1.489	5.344	6.489	2.160	1.866
4.6	1.631	1.436	5.269	6.619	2.066	2.042
4.8	1.658	1.392	5.204	6.443	1.836	2.090
5.0	1.597	1.308	4.938	5.867	1.534	2.010

Table 6. Effective collision strengths for transitions within the $3s^2 3p^2$ ground configuration of Ar V

	Transition					
$\log T$ (K)	$^3P_0-^3P_1$	$^3P_0-^3P_2$	$^3P_1-^3P_2$	$^3P-^1D$	$^3P-^1S$	$^1D-^1S$
3.0	4.162	1.869	9.409	5.026	0.402	2.319
3.2	3.959	1.871	9.159	4.142	0.466	2.030
3.4	3.747	1.931	9.030	3.697	0.516	1.847
3.6	3.519	1.979	8.852	3.456	0.540	1.745
3.8	3.257	1.953	8.465	3.281	0.550	1.685
4.0	2.941	1.837	7.811	3.207	0.559	1.648
4.2	2.582	1.672	6.989	3.319	0.585	1.649
4.4	2.240	1.514	6.207	3.622	0.637	1.688
4.6	1.981	1.407	5.642	4.043	0.698	1.742
4.8	1.816	1.349	5.305	4.401	0.733	1.775
5.0	1.682	1.285	4.994	4.454	0.710	1.741

Table 7. Effective collision strengths for transitions within the $3s^2 3p^2$ ground configuration of K VI

	Transition					
$\log T$ (K)	$^3P_0-^3P_1$	$^3P_0-^3P_2$	$^3P_1-^3P_2$	$^3P-^1D$	$^3P-^1S$	$^1D-^1S$
3.0	0.830	1.146	3.615	4.673	1.370	2.435
3.2	0.976	1.242	4.015	4.725	1.331	2.086
3.4	1.043	1.271	4.163	4.977	1.203	1.818
3.6	1.049	1.260	4.146	5.153	1.032	1.667
3.8	1.047	1.234	4.084	5.047	0.883	1.636
4.0	1.071	1.196	4.030	4.721	0.787	1.671
4.2	1.126	1.161	4.020	4.383	0.735	1.692
4.4	1.214	1.154	4.113	4.196	0.711	1.680
4.6	1.333	1.181	4.323	4.168	0.690	1.675
4.8	1.449	1.219	4.554	4.169	0.658	1.680
5.0	1.505	1.223	4.632	4.031	0.606	1.642

Table 8. Effective collision strengths for transitions within the $3s^2 3p^2$ ground configuration of Ca VII

	Transition					
$\log T$ (K)	$^3P_0-^3P_1$	$^3P_0-^3P_2$	$^3P_1-^3P_2$	$^3P-^1D$	$^3P-^1S$	$^1D-^1S$
3.0	1.258	0.954	3.718	6.152	0.611	0.634
3.2	1.264	1.004	3.839	5.042	0.752	0.660
3.4	1.282	1.041	3.944	4.242	0.903	0.660
3.6	1.259	1.035	3.902	3.883	0.984	0.639
3.8	1.194	0.998	3.739	3.960	0.959	0.619
4.0	1.153	1.005	3.702	4.245	0.865	0.633
4.2	1.215	1.129	4.059	4.434	0.762	0.723
4.4	1.369	1.318	4.676	4.398	0.680	0.883
4.6	1.512	1.455	5.163	4.196	0.618	1.048
4.8	1.589	1.497	5.354	3.897	0.562	1.159
5.0	1.594	1.453	5.263	3.515	0.502	1.197

Table 9. Effective collision strengths for transitions within the $3s^2 3p^4$ ground configuration of Ar III

	Transition					
$\log T$ (K)	$^3P_2-^3P_1$	$^3P_2-^3P_0$	$^3P_1-^3P_0$	$^3P-^1D$	$^3P-^1S$	$^1D-^1S$
3.0	3.726	0.725	1.676	5.092	0.912	1.587
3.2	3.507	0.696	1.552	5.055	0.927	1.506
3.4	3.342	0.677	1.456	5.030	0.913	1.395
3.6	3.226	0.665	1.384	4.988	0.884	1.302
3.8	3.137	0.660	1.322	4.916	0.858	1.248
4.0	3.087	0.671	1.261	4.825	0.841	1.219
4.2	3.117	0.715	1.207	4.738	0.828	1.188
4.4	3.209	0.781	1.162	4.687	0.815	1.145
4.6	3.315	0.854	1.128	4.663	0.797	1.096
4.8	3.343	0.906	1.089	4.534	0.757	1.038
5.0	3.164	0.897	1.006	4.153	0.677	0.951

Table 10. Effective collision strengths for transitions within the $3s^2 3p^4$ ground configuration of K IV

	Transition					
$\log T$ (K)	$^3P_2-^3P_1$	$^3P_2-^3P_0$	$^3P_1-^3P_0$	$^3P-^1D$	$^3P-^1S$	$^1D-^1S$
3.0	3.045	0.660	1.248	4.719	1.718	0.768
3.2	3.568	0.818	1.382	4.988	2.132	0.791
3.4	3.976	0.982	1.413	5.310	2.572	0.790
3.6	4.173	1.112	1.338	5.652	2.792	0.769
3.8	4.181	1.185	1.212	5.909	2.673	0.760
4.0	4.124	1.219	1.105	6.013	2.311	0.789
4.2	4.170	1.258	1.071	6.065	1.885	0.875
4.4	4.333	1.304	1.119	6.139	1.523	1.032
4.6	4.490	1.330	1.199	6.123	1.254	1.225
4.8	4.491	1.308	1.239	5.842	1.046	1.348
5.0	4.200	1.208	1.186	5.197	0.854	1.314

Table 11. Effective collision strengths for transitions within the $3s^2 3p^4$ ground configuration of Ca V

	Transition					
$\log T$ (K)	$^3P_2-^3P_1$	$^3P_2-^3P_0$	$^3P_1-^3P_0$	$^3P-^1D$	$^3P-^1S$	$^1D-^1S$
3.0	2.748	0.668	0.996	3.135	0.147	1.090
3.2	2.436	0.603	0.863	2.868	0.165	1.198
3.4	2.251	0.579	0.758	2.712	0.199	1.288
3.6	2.196	0.590	0.695	2.741	0.270	1.339
3.8	2.220	0.615	0.670	2.869	0.379	1.353
4.0	2.298	0.648	0.671	3.067	0.522	1.348
4.2	2.440	0.704	0.685	3.346	0.690	1.354
4.4	2.681	0.789	0.725	3.691	0.825	1.379
4.6	3.001	0.887	0.804	3.987	0.870	1.402
4.8	3.278	0.962	0.891	4.066	0.823	1.381
5.0	3.348	0.972	0.928	3.829	0.713	1.275

4. Results

The computed effective collision strengths for transitions within the ground configuration of ions in the silicon ($3s^23p^2$) and sulphur ($3s^23p^4$) sequences are listed in Tables 4–11. These data are tabulated for the electron-temperature range 10^3-10^5 K, which should cover most astrophysical applications where IR lines are studied. For transitions to the ^{1}D and ^{1}S states, we have given the sum of the fine-structure components as the latter can be obtained from the statistical weights of the ^3P_J levels from which they arise.

In the present calculation, target states from $n = 4$ configurations have been excluded from the CC expansion. Resonance series converging to such thresholds begin to appear in the energy region of interest in the low-Z members of the isoelectronic sequences, namely S III and Ar III. In order to quantify this effect, the calculation for S III was repeated including in the CC expansion the two lowest $n = 4$ states, namely $3s^23p4s\ ^{3,1}P^\circ$ that are embedded among those from the $3s3p^3$ and $3s^23p3d$ excited configurations (see Table 2). As shown in Figs. 1 and 2, the inclusion of the two lowest $n = 4$ states mainly causes an increase of the effective collision strengths in the low-temperature region for transitions to the ^{1}D and ^{1}S states; this increase is produced by a general shift of the resonance positions to lower energies (see Fig. 1). Since the differences between the two approximations for S III are not larger than 20%, and taking into account that they are expected to decrease with Z, we are confident that states from $n = 4$ configurations can be safely neglected in the CC expansion. We have not studied, however, the effect produced by taking into account more extensive $n = 4$ CI in the target wavefunctions, particularly from configurations containing 4p, 4d and 4f orbitals. These correlation effects are found to be slowly convergent for ions with open 3d shells, and therefore would lead to very large calculations.

In Fig. 3 we compare present rates for S III with the 7-state results of Mendoza (1982) for the $^3P - ^1D$, $^3P - ^1S$ and $^1D - ^1S$ transitions and with the preliminary results reported by Mendoza (1983) in a 12-state approximation. In the earlier work less refined target representations were used, in particular a more modest CI expansion for the excited target states where the contributions from double excitations were neglected. The agreement is found to be within 20% except with the results reported by Mendoza (1983) for the $^1D - ^1S$ transition where differences are as high as 40%. The sensitivity of the quadrupole transition to target description has been previously reported in the comparative work on the electron excitation of O III by Burke et al. (1989).

Present results for Ar III are compared with the work of Johnson and Kingston (1990) in Fig. 4. The CI expansion used by those authors is more detailed in as much as they take into account configurations with 4f orbitals; however, they only include in the CC expansion the 5 terms arising from the $3s^23p^4$ and $3s3p^5$ configurations. In the present work, terms arising from the configurations $3s^23p^33d$ and $3p^6$ are also considered. In spite of the different treatments, the agreement can be seen to be within 10%.

In the compilation by Mendoza (1983), preliminary results are also given for the LS coupling transitions in Cl IV and Ar V. While the agreement for the former is within

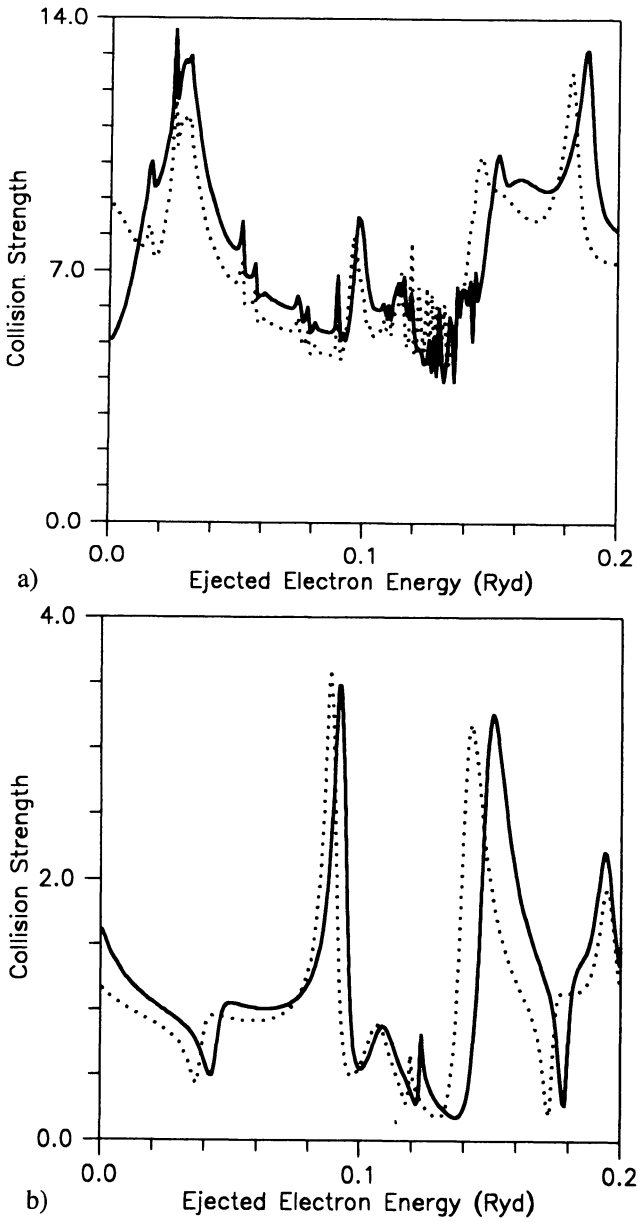

Fig. 1. Collision strengths in the near-threshold region for the a) $^3P - ^1D$ and b) $^1D - ^1S$ transitions in S III. The dotted line shows the results obtained when the $3s^23p4s\ ^{3,1}P^\circ$ target states are included in the CC expansion. It is shown that the inclusion of such $n = 4$ states can cause significant shifts of the resonance positions

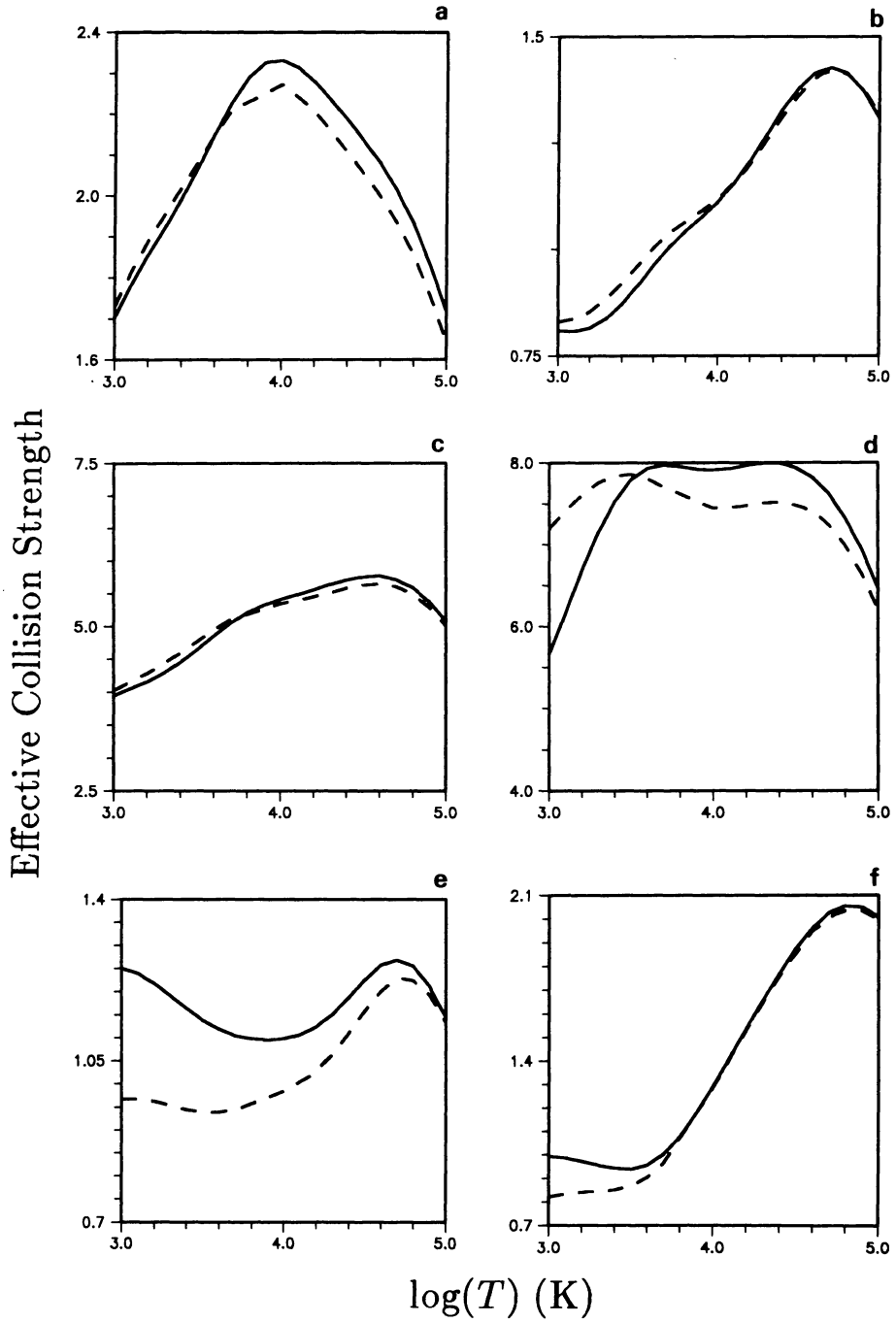

Fig. 2. Effective collision strengths for transitions within the ground configuration of S III. a) $^3P_0-^3P_1$; b) $^3P_0-^3P_2$; c) $^3P_1-^3P_2$; d) $^3P-^1D$; e) $^3P-^1S$; f) $^1D-^1S$. The dashed curve shows the results obtained when the $3s^23p4s\ ^{3,1}P^\circ$ states are included in the CC expansion. It can be seen that the larger differences occur in the low-temperature region for transitions to the ^1D and ^1S terms; as shown in Fig. 1, such changes are due to the lowering of resonance positions

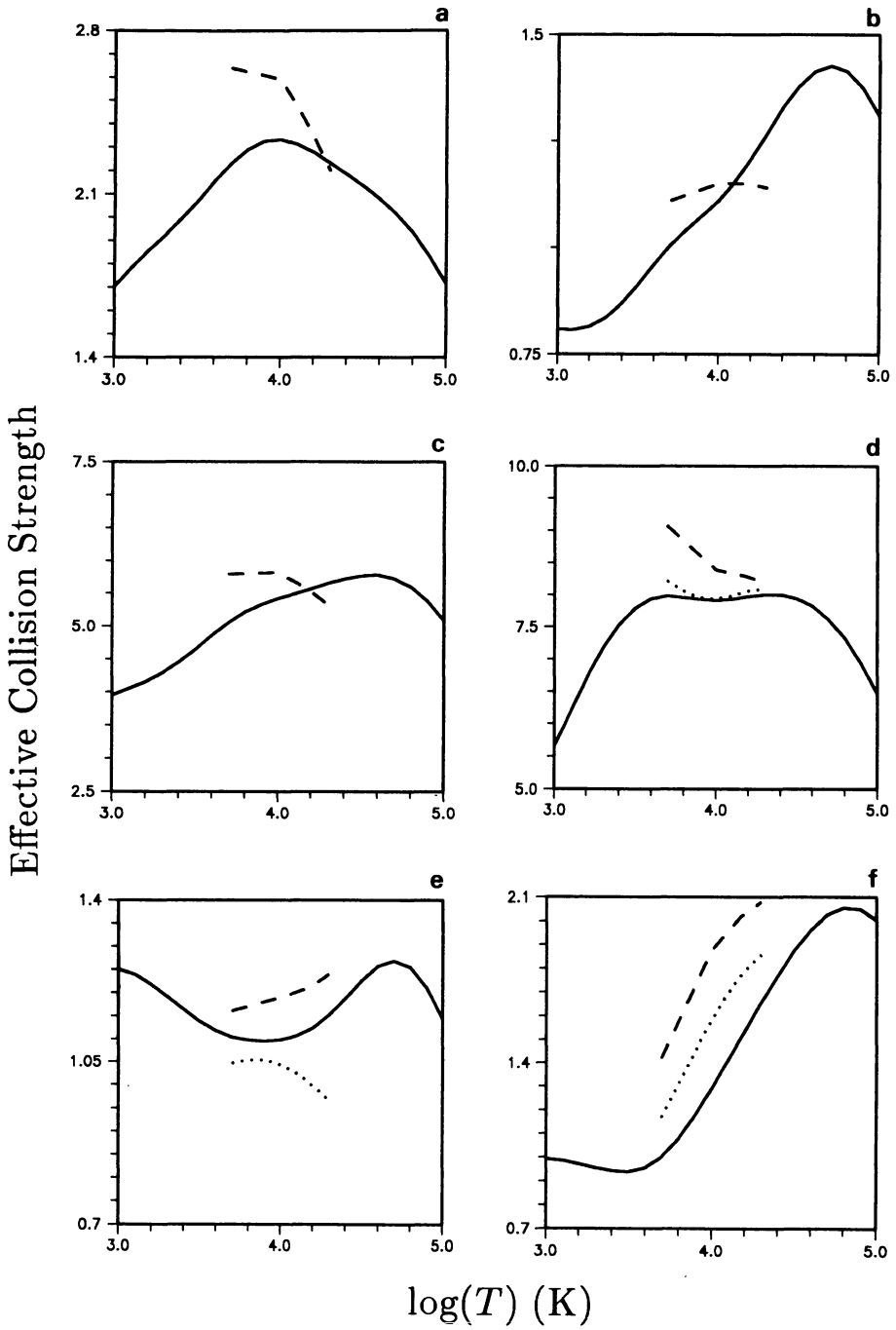

Fig. 3. Comparison of present effective collision strengths for transitions within the ground configuration of S III (solid curve) with the CC results reported by Mendoza (1982) in a 7-state (dotted curve) and Mendoza (1983) in a 12-state (dashed curve). a) $^3P_0-^3P_1$; b) $^3P_0-^3P_2$; c) $^3P_1-^3P_2$; d) $^3P-^1D$; e) $^3P-^1S$; f) $^1D-^1S$. The discrepancies are due to the different target representations used in the calculations; the present is the most elaborate used to date, and therefore should yield the most reliable rates

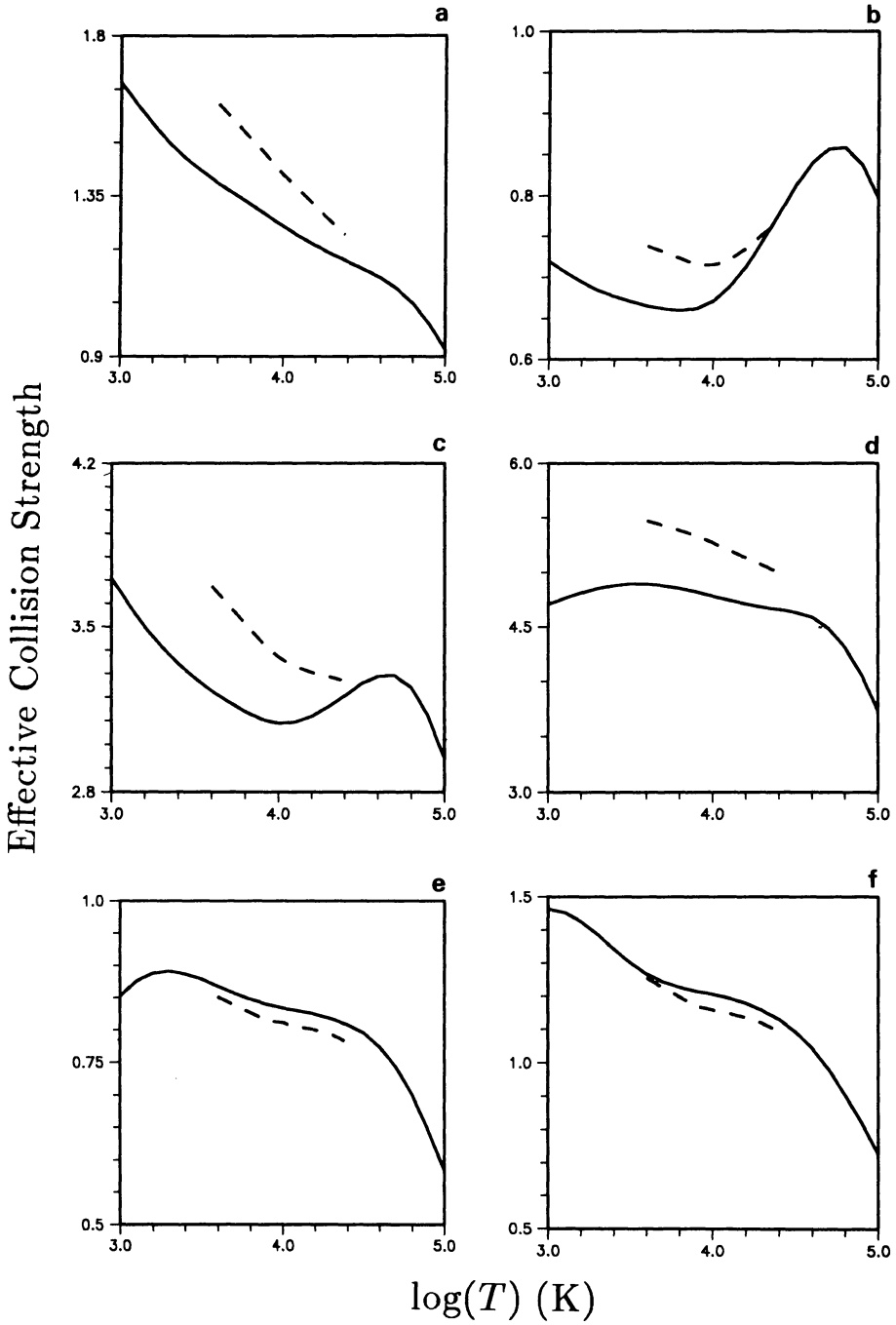

Fig. 4. Comparison of present effective collision strengths for transitions within the ground configuration of Ar III (solid curve) with the CC results by Johnson & Kingston (1990) (dashed curve). a) $^3P_1-^3P_0$; b) $^3P_2-^3P_0$; c) $^3P_2-^3P_1$; d) $^3P-^1D$; e) $^3P-^1S$; f) $^1D-^1S$. The overall agreement between the two independent calculations is good even though the authors of the earlier work used a much simpler target approximation

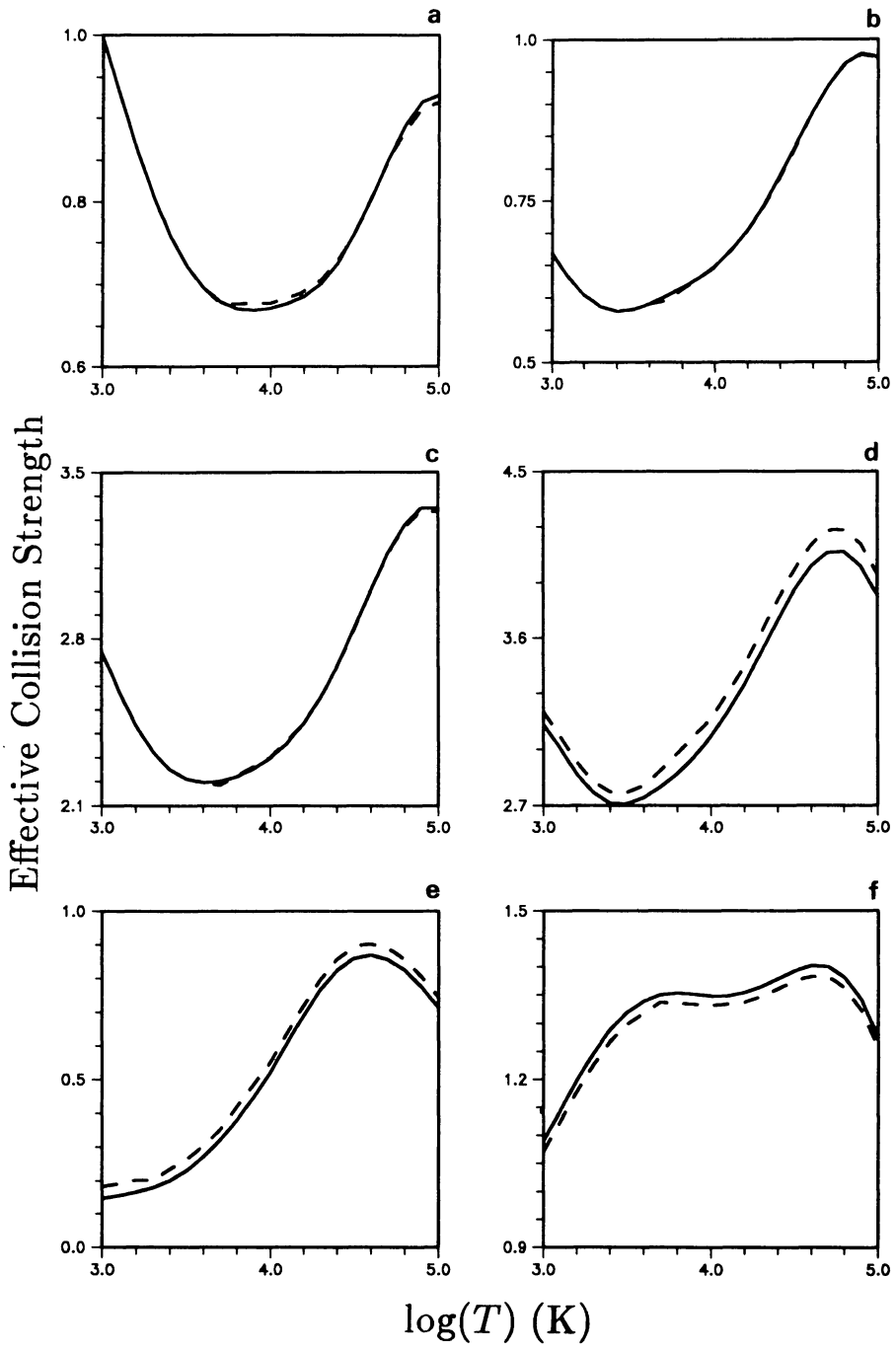

Fig. 5. Comparison of present effective collision strengths for transitions within the ground configuration of Ca V (solid curve) with those obtained by including relativistic target effects (dashed curve). a) $^3P_1-^3P_0$; b) $^3P_2-^3P_0$; c) $^3P_2-^3P_1$; d) $^3P-^1D$; e) $^3P-^1S$; f) $^1D-^1S$. It can be seen that the relativistic effects are small for all the transitions considered

20% larger differences are found for the transitions to the ^1S term in Ar V, in particular, a discrepancy of a factor of 2 in the $^1D-^1S$ transition. This is a clear indication of the sensitivity of some rates to the position of the resonances, particularly in the near-threshold region. Accurate resonance patterns can only be obtained through sound target representations that at present cannot be obtained due to the lack of the supporting spectroscopic data. As illustrated with the case of Ar V, this problem should become more evident for the higher members of the sequences due to the exclusion of an increasing number of contributing thresholds for which it is not possible at present to obtain reliable energy positions.

Relativistic effects in the target are studied in the excitation of Ca V (Fig. 5). It can be seen that, although the transitions within the ^3P_J ground state are hardly affected, the transitions to the higher states show some small differences ($\sim$ 5%): the effective collision strengths for the transitions from the ^3P ground state to the ^1D and ^1S states are increased while that for the ^1D–^1S transition decreases. In the light of those results, relativistic effects have been neglected in this work.

5. Conclusions

We have presented effective collision strengths for electronic impact excitation of states within the ground configuration of ions in the Si and S isoelectronic sequences which cover the temperature range of interest; they are expected to be the most reliable to date. The accuracy of the data for the weakly ionised members is estimated to be within 20% based on the good agreement found for S III and Ar III with previous work. On the other hand, the accuracy in the case of the higher members is expected to be lower due to the impossibility of building target descriptions of suitable size and accuracy because of the general lack of the required spectroscopic data for these sequences. We would therefore welcome further measurements since future computational attempts will not be able to get round the present deficiency, particularly in the treatment of the corresponding ions of Fe which is the central objective of the Project.

Acknowledgements. The present computations were performed on the CRAY YMP at the Ohio Supercomputer Center (OSC), Columbus, Ohio, U.S.A., via the Venezuelan academic network (SAICYT) and on the IBM 3090 at the IBM Venezuela Computing Center. The authors are very much indebted to Prof. Anil Pradhan and Dr. Honglin Zhang from the Ohio State University for assistance in running the R-matrix suite of codes at the OSC, particularly their recent implementation of the asymptotic module that handles intermediate coupling. During the 1992–94 period, the present collaboration has benefited from visits by MEG and CM to the Observatoire de Paris, Meudon, France, and by CJZ to the IBM Venezuela Scientific Center. The visits were funded by the CNRS, the CONICIT, the Observatoire de Paris and IBM Venezuela.

References

Berrington K.A. 1995, A&AS 109, 193
Burke P.G., Hibbert A., Robb W.D. 1971, J. Phys. B 4, 153
Burke P.G., Seaton M.J. 1971, Meth. Comp. Phys. 10, 1
Burke V.M., Lennon D.J., Seaton M.J. 1989, MNRAS 236, 353
Butler K., Zeippen C.J. 1994, A&AS 108, 1
Corliss C., Sugar J. 1979, J. Phys. Chem. Ref. Data 8, 1109
Eissner W. 1991, J. Phys. IV C1, 3
Eissner W., Jones M., Nussbaumer H. 1974, Comput. Phys. Commun. 8, 270
Hummer D.G., Berrington K.A., Eissner W. et al. 1993, A&A 279, 298 (Paper I)
Jones M. 1975, Phil. Trans. Roy. Soc. London 277, 588
Johnson C.T., Kingston A.E. 1990, J. Phys. B 23, 3393
Lang J. (Special Editor) 1994, At. Data Nucl. Data Tables 57, 1
Lennon D.J., Burke V.M. 1994, A&AS 103, 273
Martin W.C., Zalubas R., Musgrove A. 1990, J. Phys. Chem. Ref. Data 19, 821
Mendoza C. 1982, J. Phys. B 15, 867
Mendoza C. 1983, Proc IAU Symposium 103, ed. D.R. Flower (Dordrecht: Reidel) 142
Moore C.E. 1971, Atomic Energy Levels NSRDS-NBS35. US Govt. Printing Office, Washington, DC
Nahar S.N. 1995, A&A 293, 967
Nussbaumer H., Storey P.J. 1978, A&A 64, 139
Pelan J., Berrington K.A. 1995, A&AS 110, 209
Pradhan A.K., Gallagher J.W. 1992, At. Data Nucl. Data Tables 52, 227
Pradhan A.K., Zhang H.L. 1994, private communication
Saraph H.E. 1972, Comput. Phys. Commun. 3, 256
Saraph H.E. 1978, Comput. Phys. Commun. 15, 247
Saraph H.E., Tully J.A. 1994, A&AS 107, 29
Seaton M.J. 1985, J. Phys. B 18, 2111
Sugar J., Corliss C. 1979, J. Phys. Chem. Ref. Data 8, 865
Zhang H.L., Graziani M., Pradhan A.K. 1994, A&A 283, 319
Zhang H.L., Pradhan A.K. 1995, A&A 293, 953